ANOTHER LOOK AT THE EUROPEAN BLOCK OF FEBRUARY 1986

Prashant D. Sardeshmukh
European Centre for Medium-range Weather Forecasts
Reading, United Kingdom

1. INTRODUCTION

The end of January 1986 marked a rapid transition to a pronounced blocked flow regime over the north east Atlantic with part of NW Europe having its coldest February in 300 years. January itself, as well as the previous December, had however been mild in the same region with the anomalies confined mostly to the Pacific sector. Such an extreme change of flow regime within a single winter season is unusual, and proved difficult to capture in operational medium range weather forecasts. Hoskins and Sardeshmukh (1987) have recently discussed the differences in the large-scale circulation between the two parts of the winter, with a view of identifying the possible cause for those differences. Their detailed diagnosis will not be repeated here. Rather, we shall summarize their principal conclusions and append some additional evidence in support.

2. GENERAL DIAGNOSTICS

The mean streamfunction anomalies at 250 mb, determined as deviations from a six-year December-January-February (DJF) average, are shown in Fig. 1 for the average of December and January (a) and for February (b). Consistent with the equivalent barotropic nature of large-scale anomalies on such time scales (Wallace and Gutzler, 1981), positive values are associated with warm and negative values with cold temperature anomalies in the lower troposphere (not shown). The early winter is characterized by a pattern of alternating positive and negative anomalies that is suggestive of a wave-train emanating from the subtropical western Pacific. In February this pattern is replaced by a zonally elongated dipole in the N.Pacific. However, the major change is the appearance of the blocking pattern in the Atlantic/European sector.

Figure 1 also shows the corresponding anomaly maps for the two halves of February. They are generally similar over much of the hemisphere except over western N.America, where the flow across the Rockies undergoes an extreme

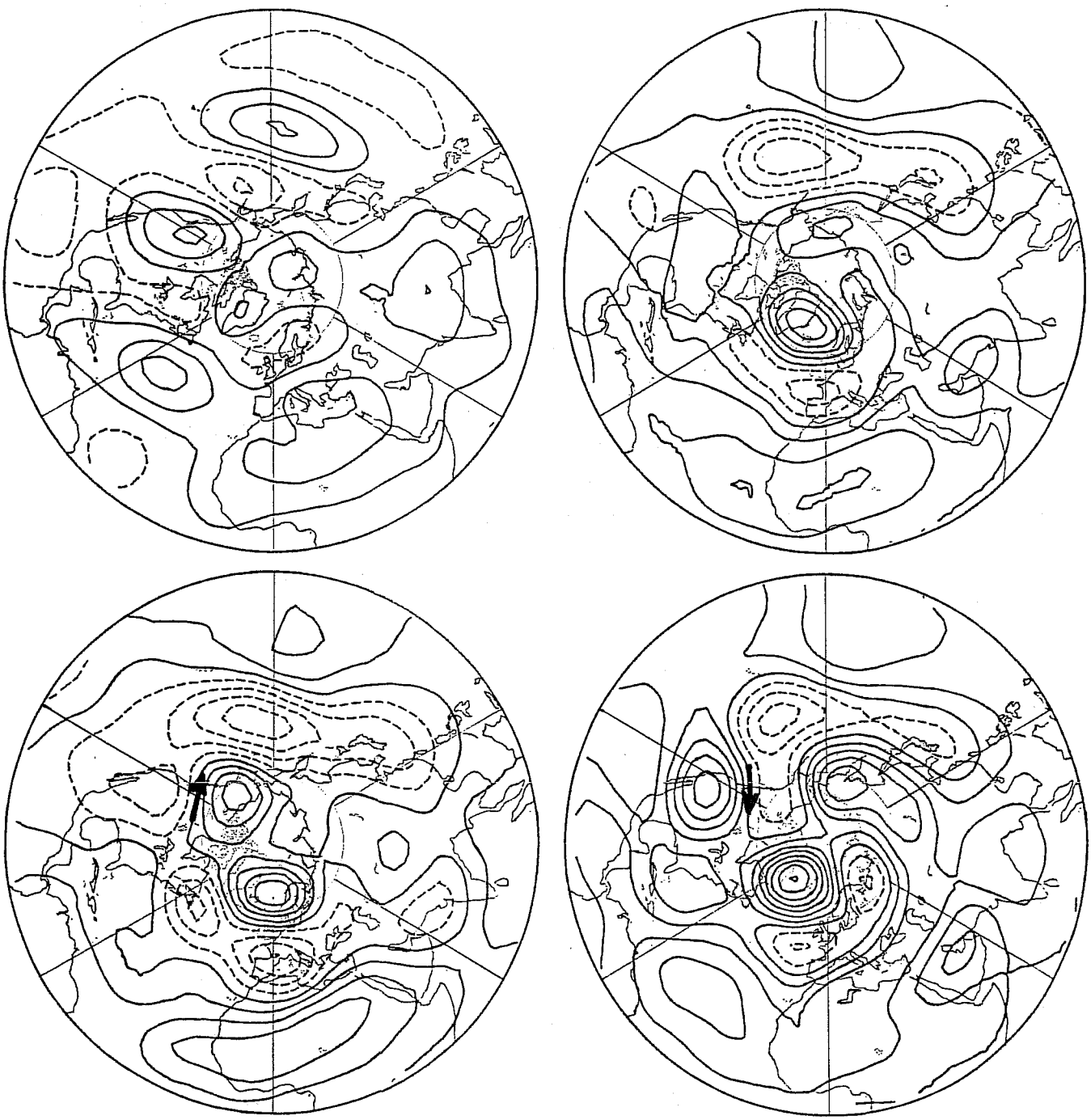

Fig. 1 Mean 250 mb streamfunction anomalies for (a) December 85 + January 86 (upper left), (b) February 86 (upper right), (c) 1-15 February 86 (lower left), and (d) 16-28 February 86 (lower right), all determined as deviations from a six-year (1979-84) DJF average as given by the ECMWF operational analyses. The contour interval is 5 x 10^6 m^2 s^{-1} and negative contours are dashed. Adapted from Hoskins and Sardeshmukh (1987).

change from a strong anomalous easterly flow in the first half of the month to strong westerly in the second, and yet the blocking signature over the Atlantic is hardly affected. Thus in this case the interaction of the flow with the Rockies appears an unlikely mechanism for the blocked flow downstream.

Shutts (1986), Hoskins et al. (1985), and others have discussed the dynamics of blocks in terms of the evolution of potential vorticity (PV) on isentropic surfaces. According to this view, the essential ingredient of a blocking high is a large poleward excursion of low PV subtropical air ahead of a slowly moving, meridionally elongated trough that is usually associated with decaying synoptic systems, and is thus most likely to occur at the end of a storm-track where there is already a tendency for the flow to split. This anomalous low PV air tends to develop its own anticyclonic circulation which then cuts it off from its source region. Given the conservative properties of PV, the only way for such an anticyclone to decay is by moving back to the subtropics or by diabatic processes, which in such instances would probably involve only radiative cooling, acting on the time scale of a week or more.

Although the mean PV map for February 1986 on the 315 K isentropic surface does indeed show closed contours of PV in the blocked region, inspection of the daily maps suggests a more complex picture. There were altogether nine separate events in the month in which a cut-off low of PV ahead of decaying mobile trough renewed the blocking system. Indeed the slight westward shift of the block in the second half of the month (see Fig 1) was almost certainly related to a major synoptic development that occurred on February 16, further west than usual, close to the east coast of N.America where the surface pressure minimum deepened to 960 mb in 12 hours. The maintenance of this blocked regime was thus intimately tied to the behaviour of the synoptic systems upstream.

3. THE IMPORTANCE OF SYNOPTIC TIME-SCALE TRANSIENTS

Given the presence of a block, the different behaviour of synoptic systems in the region is perhaps to be expected; the question is whether that difference is crucial for the existence of the block. Hoskins and Sardeshmukh addressed this issue with a diagnostic vorticity equation model. Separating the mean horizontal flow $\underset{\sim}{\bar{V}}$ at some upper tropospheric level such as 250 mb into its

rotational and divergent components, $\bar{\underset{\sim}{V}}_\psi$ and $\bar{\underset{\sim}{V}}_\chi$, the vertical component of the time-mean vorticity equation may be written

$$[\bar{u}]\,\frac{\partial \bar{\zeta}^*}{\partial x} + \bar{\underset{\sim}{V}}_\psi{}^* \cdot \underset{\sim}{\nabla}\,([\bar{\zeta}] + \bar{\zeta}^*) = -\,\bar{\underset{\sim}{V}} \cdot \{\bar{\underset{\sim}{V}}_\chi\,([\bar{\zeta}] + \bar{\zeta}^*)\} - \underset{\sim}{\nabla} \cdot \overline{\underset{\sim}{V}'\zeta'} + F \qquad (1)$$

where an overbar refers to a time mean, a prime to a deviation from it, a square bracket to a zonal mean, an asterisk to a deviation from it, u to the zonal velocity and ζ to the absolute vorticity $\zeta = f + \underset{\sim}{k} \cdot \underset{\sim}{\nabla} \times \underset{\sim}{V}_\psi$. F represents the sum of the vertical advection, twisting, and frictional terms, which was modelled as a simple linear drag plus a small biharmonic diffusion, both acting on the zonally asymmetric vorticity $\bar{\zeta}^*$.

If one specifies from observations (i) the time-mean, zonal-mean zonal flow $[\bar{u}]$, (ii) the time-mean divergent flow $\bar{\underset{\sim}{V}}_\chi$, and (iii) the transient vorticity flux convergence $-\underset{\sim}{\nabla} \cdot \overline{\underset{\sim}{V}'\zeta'}$, there is only one unknown $\bar{\psi}^*$ in this equation as $\bar{\underset{\sim}{V}}_\psi{}^* = \underset{\sim}{k} \times \underset{\sim}{\nabla}\,\bar{\psi}^*$ and $\bar{\zeta}^* = \nabla^2\,\bar{\psi}^*$. To solve this equation a term $\partial\bar{\zeta}^*/\partial t$ is added on the left hand side and the equation is integrated forward in time until a steady state is reached. The time-mean, zonally asymmetric streamfunction $\bar{\psi}^*$ thus obtained should be close to that observed if the data are consistent and if the modelling of F is correct. Numerous such tests have been carried out on the ECMWF analyses with very encouraging results. It seems likely that when errors exist they are primarily due to errors in the analysis of the divergent flow.

Such calculations were carried out separately for February and for the previous two-month period of December+January. Figs 2a and 2b show the difference $\psi_{FEB} - \psi_{DEC+JAN}$ for the observations and for the model. As discussed above, the similarity of the two amounts to little more than a consistency check (albeit a powerful one) on the ECMWF analyses. However, when the term involving the transient vorticity fluxes is omitted from the simulation for both periods, the same field (Fig 2c) is dramatically different. The blocking signature in the eastern Atlantic is now totally missing. The change in the transient eddies is clearly crucial to the change from the December+January mean flow to the February mean flow. At the same time, the simulations do not show such sensitivity to the change in the zonal mean zonal flow from one period to the other.

Studying the daily PV maps and also the E-vector diagnostics (Hoskins et al., 1983) strongly suggests that the crucial change is predominantly in the synoptic time-scale transients rather than a manifestation of one of the low-frequency barotropic modes of Simmons et al. (1983). Of course, if such a change is totally internal to the middle latitude atmosphere then it is inherently unpredictable. Also, one is not any the wiser as to why the block should occur at all.

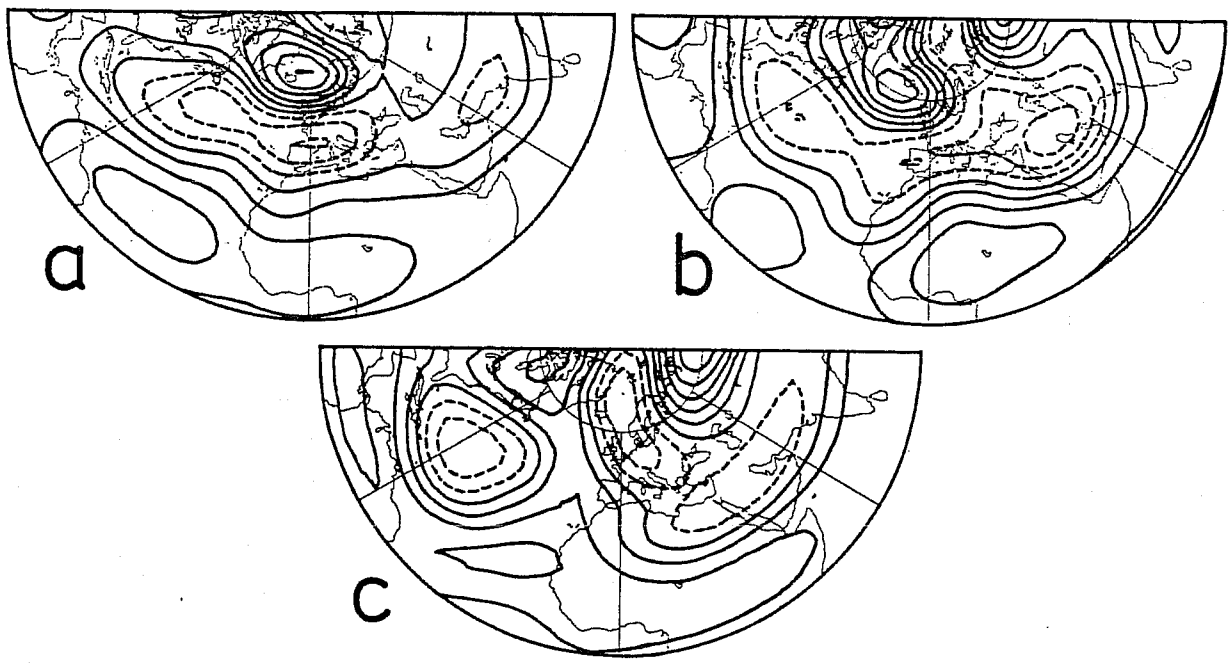

Fig. 2 The change in the 250 mb streamfunction from December+January to February 86 for (a) the observations, (b) the full vorticity equation model, and (c) the vorticity equation model with zero transient vorticity flux convergence for both periods. Contouring as in Fig 1. From Hoskins and Sardeshmukh (1987).

4. OTHER INFLUENCES

Further progress is possible if one could link the occurrence of blocks to 'external' (or perhaps more accurately, to 'independent') effects. The primary candidates for these are orographic forcing and diabatic heating. As discussed above, the variety of the half-monthly average flows in the region of the Rockies did not support the idea that this block could have been the result of a resonant interaction with mountain forcing. Hoskins and Sardeshmukh also examined time-mean maps of the vertically integrated diabatic heating (not shown here) calculated as a residual in the thermodynamic

equation using ECMWF analyses. In middle latitudes the dominant change from the earlier part of the winter to February was a confinement of the N.Atlantic heating to the west, thereby implying a different forcing of the mean flow in February. It is true that much of this heating is associated with latent heat release in synoptic systems; and so the change should probably be viewed as a signature of the truncated storm track, rather than a cause of the differing weather regimes.

On the other hand, both the column-integrated diabatic heating and the upper-level divergence fields showed interesting differences between the two periods in the tropics. However, the significance of some of these, particularly in the Indonesian region connected with the 40 to 50 day oscillation, could not be assessed in detail owing to the lack of adequate climatological data. More emphasis was placed on the enhanced cooling that occurred in association with reduced cloudiness and rainfall over the Caribbean area in February. Consistent changes were seen in the 250 mb divergence field, essentially amounting to an intensification of the local Hadley circulation over the tropical Atlantic. Sensitivity experiments conducted with the diagnostic vorticity equation model showed a tendency for weak anticyclonic flow to become established over the north Atlantic in association with these changes. It is possible that this provided the catalyst that made the blocking process, in which the transients are vital, much more likely to occur.

It is not yet clear as to why the divergence should have been different over the tropical American region. The sea surface temperature (SST) charts in the Climate Analysis Center Bulletins (1985,1986a,b) do show a region of colder than normal water in the Caribbean and anomalously warm water in the S.Atlantic throughout the winter period; however, the block occurred only in February. Hoskins and Sardeshmukh suggested that it was the phase of the SST anomalies relative to the ITCZ, rather than the SST anomalies themselves, that was relevant. Thus the SST effect was likely to be felt relatively suddenly in the later part of the winter when the southward seasonal migration of the rainfall brought it in phase with the warm SST anomalies.

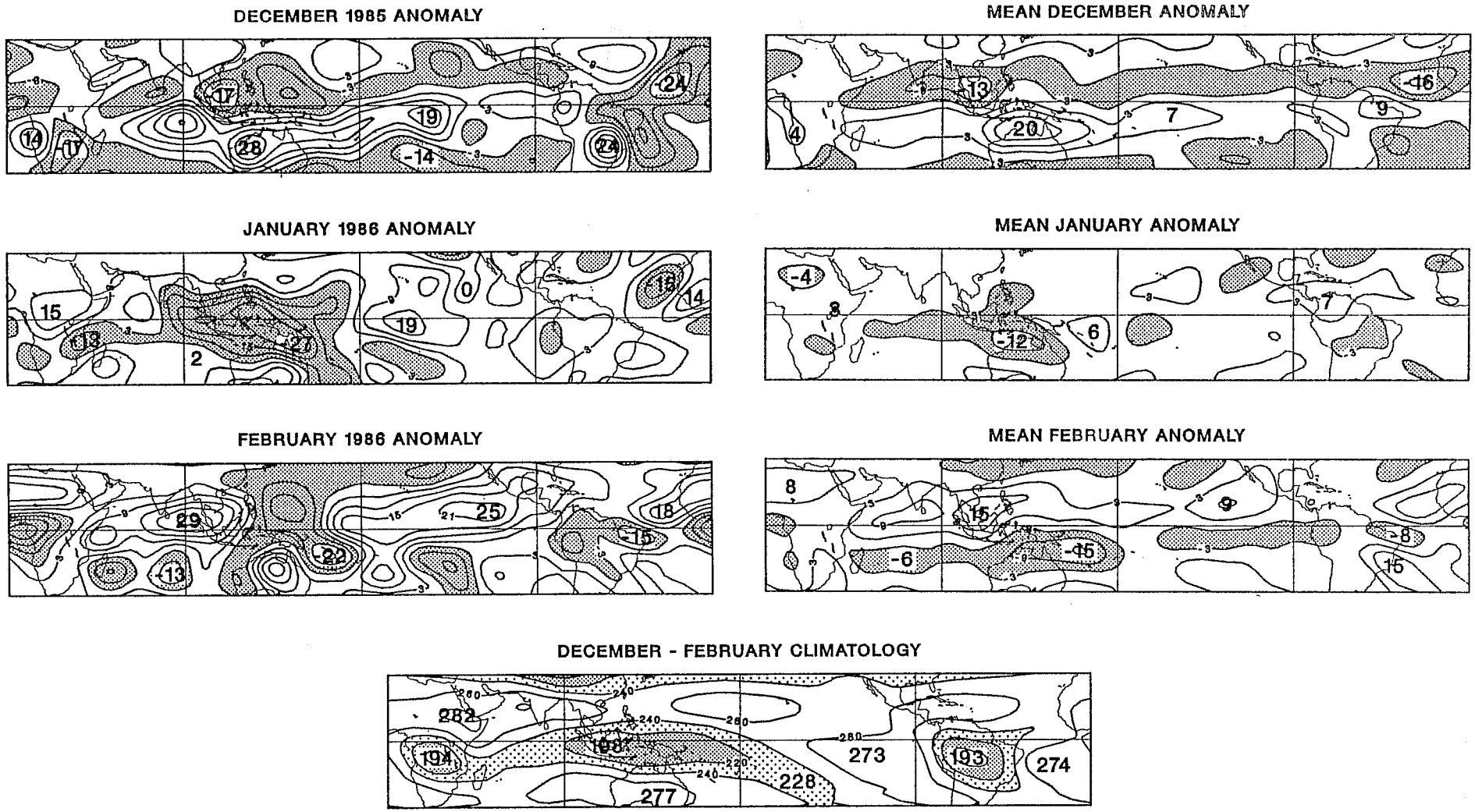

Fig. 3 Mean anomaly maps of Outgoing Longwave radiation (OLR). The word anomaly in this figure refers to deviations from a seven-year (1981-87) DJF mean OLR field shown in the bottom panel. Thus 'Mean December Anomaly' is the 7-year December mean minus the 7-year DJF mean. The contours drawn are ±3, ±9, ±15, ±21... W/m^2 and values of less than -3 W/m^2 indicating increased cloudiness are shown shaded. The fields have been spatially smoothed in the manner described by Sardeshmukh and Hoskins (1984) to show information only on scales larger than corresponding to spherical wavenumber n=21.

5. THE EVIDENCE FROM SATELLITE DATA

In the following the role of the tropics will be explored in somewhat greater detail, making use of Outgoing Longwave Radiation (OLR) data kindly made available by the Climate Analysis Center in Washington, USA. Figure 3 shows the mean OLR for the three individual months of the 1985-86 winter alongside the climatology for those months. In order to facilitate comparison and also to get a clearer view of the seasonal cycle, a seven-year (1981-87) DJF mean OLR field shown at the bottom has been subtracted from all the six panels. The southward migration of the ITCZ with the progress of the season is seen clearly in the climatological maps, with the local OLR change from December to February amounting to as much as 25 watts per square meter over the western Pacific and the tropical Atlantic. The panels for the 1985-86 winter show that much of the change over the tropical Atlantic can indeed be viewed as an intensification of the seasonal signal, consistent with the suggestion made above.

The values just north of the equator over the western Pacific and Indian oceans also look substantially different from climatology throughout the winter period. In fact these monthly-mean fields give a distorted view of the significant convective activity which occurred in that region on the 40 to 50 day time scale. A clearer picture of the low-frequency subseasonal variability is obtained by operating on the complete 7-year OLR record with a 91-point Lanczos filter (Duchon, 1979) that passes periods between 26 and 80 days. The variance of the OLR in this time band for the 21 winter months of December, January, and February in the record is shown in Figure 4. Note that

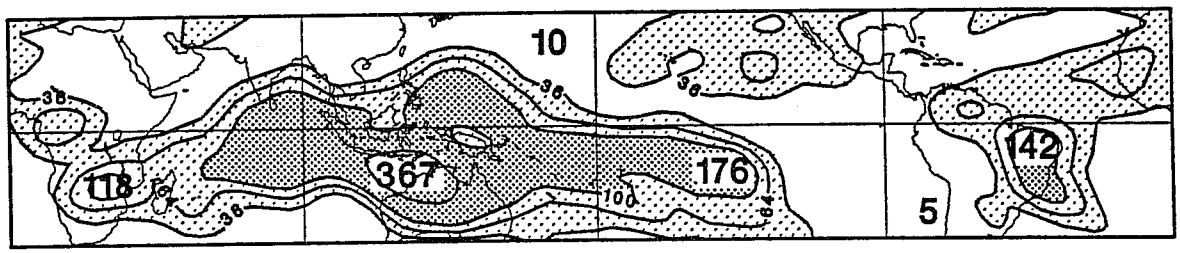

Fig. 4 Variance of OLR on the 26 to 80 day time scale for the winter (DJF) months based on data for the years 1981-87. The contours shown are 36, 64, 100, 225, 400... W^2/m^4. Values in excess of 36 W^2/m^4 are indicated by shading; those greater than 100 W^2/m^4 by heavier shading.

in addition to the large variability over the principal areas of convection (see the bottom panel of Fig 3), there are large values in the equatorial belt as well. Figure 5 shows the time-longitude section of the filtered OLR averaged between 10 N and 10 S for 120 days of the 1985-86 winter starting 15 November. For comparison the same sections for two other winters are also shown. Much of the variability in the region 60 E - 180 E is associated with the 40 to 50 day oscillation. As seen in these sections the interannual variability of the oscillation is large; also, the oscillation does not appear to be locked to the seasonal cycle. The eastward propagating component is clearly strong but in the 1985-86 winter a substantial standing component is also evident. Note the strong event that occurred in the January of this winter. At present the effects of such events on the middle latitude circulation are poorly understood but considering the peak-to-peak amplitude

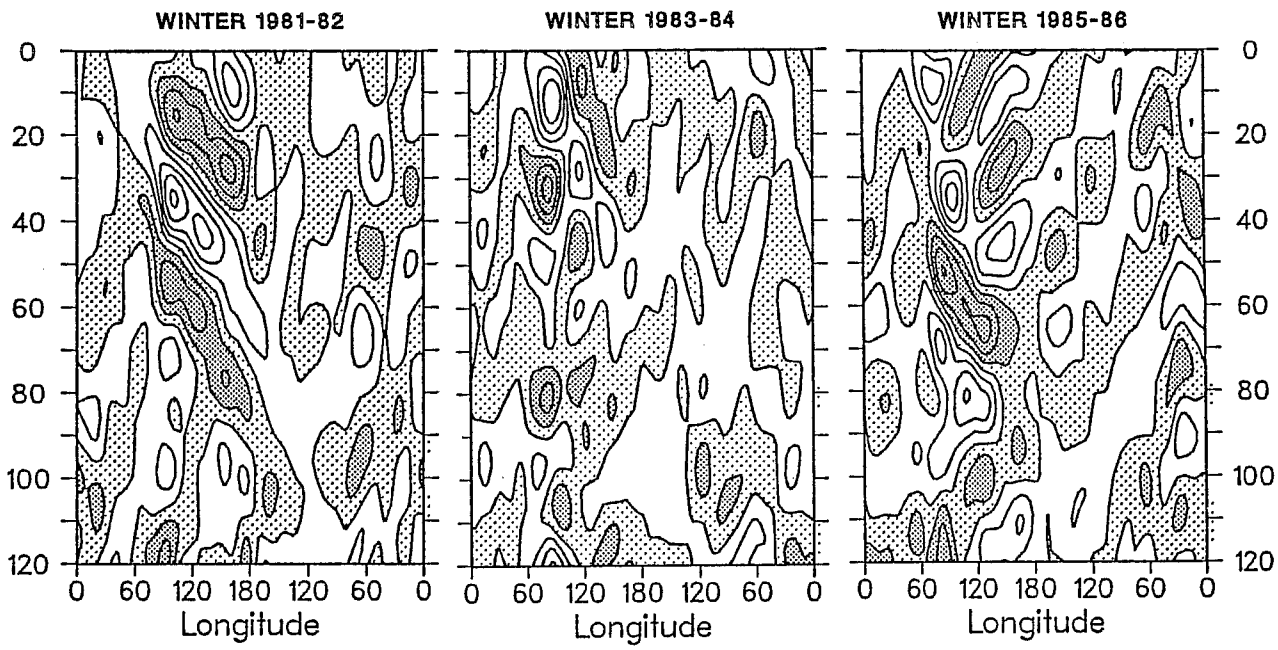

Fig. 5 Longitude-time sections of the bandpass-filtered OLR averaged between 10 N - 10 S for 120 days of the northern winter starting 15 November, for three different winters. The contour interval is 8 W/m^2. Negative values are indicated by shading, with heavier shading for values of less than -8 W/m^2.

of nearly 40 W/m^2 over large areas, they are probably not small. Weickmann et al. (1985) have given evidence of the global nature of the upper tropospheric streamfunction anomalies that are on average associated with such events.

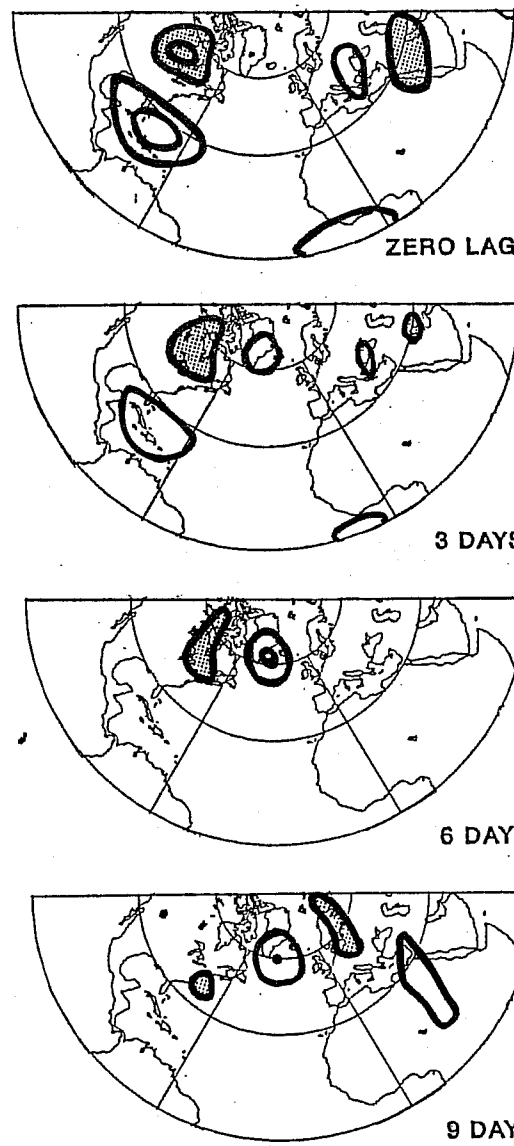

Fig. 6

The correlation of the bandpass-filtered 250 mb streamfunction in the northern hemisphere with the bandpass-filtered OLR at the reference point 20N,65W. The maps are given for several time lags of the streamfunction field with respect to the OLR time series at the reference point. Contours drawn are ±0.3, ±0.5, ±0.7,...etc and negatively contoured regions are shown shaded. Lines of longitude and latitude are drawn every 60 and 30 degrees respectively. The bounding semicircle is the equator.

It is easier to establish the link between enhanced cooling over the Caribbean and a tendency for ridging to develop over the northern Atlantic. For this study an identical seven-year time series of the 250 mb streamfunction given by the ECMWF analyses was similarly filtered to isolate the subseasonal variability on the 26 to 80 day time scale. The filtered time series at every point on the globe was then correlated with the OLR time series at the Caribbean point 20 N, 65 W. Figure 6 gives these one-point correlation maps for the wintertime fluctuations, for zero time lag between the OLR and streamfunction time series and also for the streamfunction lagging the OLR by 3, 6, and 9 days. The contours shown are ±0.3, ±0.5, ±0.7... etc and negative correlations are indicated by shading. The sign convention is such as to depict the streamfunction patterns that are associated with positive OLR, hence enhanced cooling, over the reference point.

The simultaneous correlation map shows a dipole structure over the western Atlantic with a large anticyclone over the Caribbean and a slightly weaker cyclone to its north over Hudson Bay, consistent with a tendency for a stronger than normal Atlantic jet. There is some evidence of these features being associated with an equatorward propagating wave-train from the north-east Pacific (not shown, but see Blackmon et al., 1984). However, if there is now to be evidence of any meridional dispersion and propagation of wave activity out of the tropics, one should expect these centres to weaken with time and new ones to appear further down a ray path emanating from the tropics (Hoskins and Karoly, 1981). By day 3 an additional high has indeed appeared over the northern Atlantic, just east of Greenland. This high has intensified by day 6; the low over Hudson Bay has weakened further and the Caribbean high has disappeared. By day 9 the north Atlantic high has started to weaken but additional centres have now appeared over Finland and the eastern Mediterranean.

Further experimentation with the vorticity equation model (not shown) confirms that the time scale for the energy dispersion as indicated by these lag-correlation statistics is indeed what one expects from simple theory.

Is the Caribbean region special ? A partial answer is given by performing a reverse calculation, that is, by correlating the filtered streamfunction time series at the north Atlantic point 60 N,30 W (see Fig 6) with the OLR time

series at every point in the tropics. Figure 7 gives such lead- and lag-correlation maps. As expected from Figure 6 the correlation with the point 20 N, 65 W at Day-6 is just over 0.5, and the large values are indeed confined to the western tropical Atlantic. It is interesting to see an opposite correlation of over 0.3 at Day-8 over N.E. Brazil. This is not inconsistent with the possibility of an enhanced local Hadley circulation contributing, sometimes, to the blocking process over the northern Atlantic.

There is substantial asymmetry between the lead- and lag-correlation maps. Note that the panels on the left and right hand sides of the figure have been arranged in such a way as to show the correlations for times separated by 10 days side by side. The purpose of this is to stress that although the correlations in the western equatorial Pacific are only in the order of 0.2 - 0.3, the patterns themselves and the fact they are almost exactly in quadrature with those of 10 days later suggest a link with the 40 to 50 day oscillation. This is particularly relevant considering that the time filtering applied to the data is sufficiently broad-band so as not to isolate the variability only in the 40 to 50 day time scale (see Fig 4).

6. CONCLUDING REMARKS

Both enhanced cooling over the Caribbean and unusual activity on the 40 to 50 day time scale in the tropics may thus have a role to play in the blocking process over the north Atlantic. A final point to consider is whether there is any obvious statistical link between the two. To answer this question the band-pass filtered OLR time series at the same Caribbean reference point as above was correlated with the OLR time series at every other point in the tropics. The results are given in Figure 8 in a format similar to that of Fig 7. No well-defined correlation structures are now evident in the western equatorial Pacific. Interestingly, the simultaneous correlation map does not show a region of negative correlation over N.E. Brazil. This suggests indirectly that much of the OLR variability over the Caribbean must be associated with the equatorward propagating wave-train described by Blackmon et al.(1984). The lead correlation maps however do show a region of negative correlations. Note also here the strong asymmetry between the lead- and lag-correlation maps.

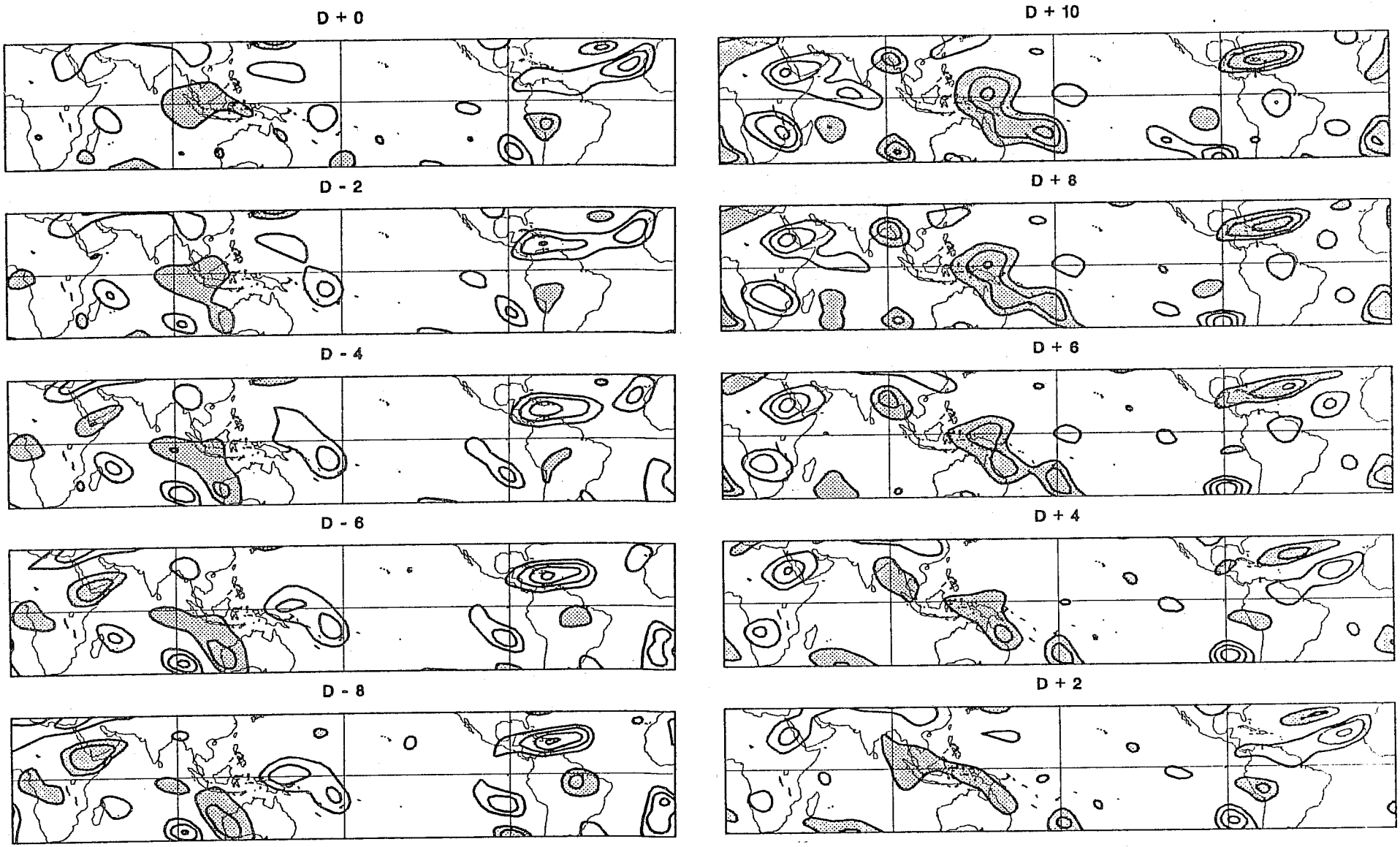

Fig. 7 Lead- and lag- correlations of the bandpass-filtered OLR time series at all the points in the tropics with the bandpass-filtered 250 mb streamfunction time series at the north Atlantic point 60N,30W, for the winter period only, based on data for the years 1981-87. The contours drawn are ±0.2, ±0.3, ±0.4,.....etc and values of less than -0.2 are indicated by shading.

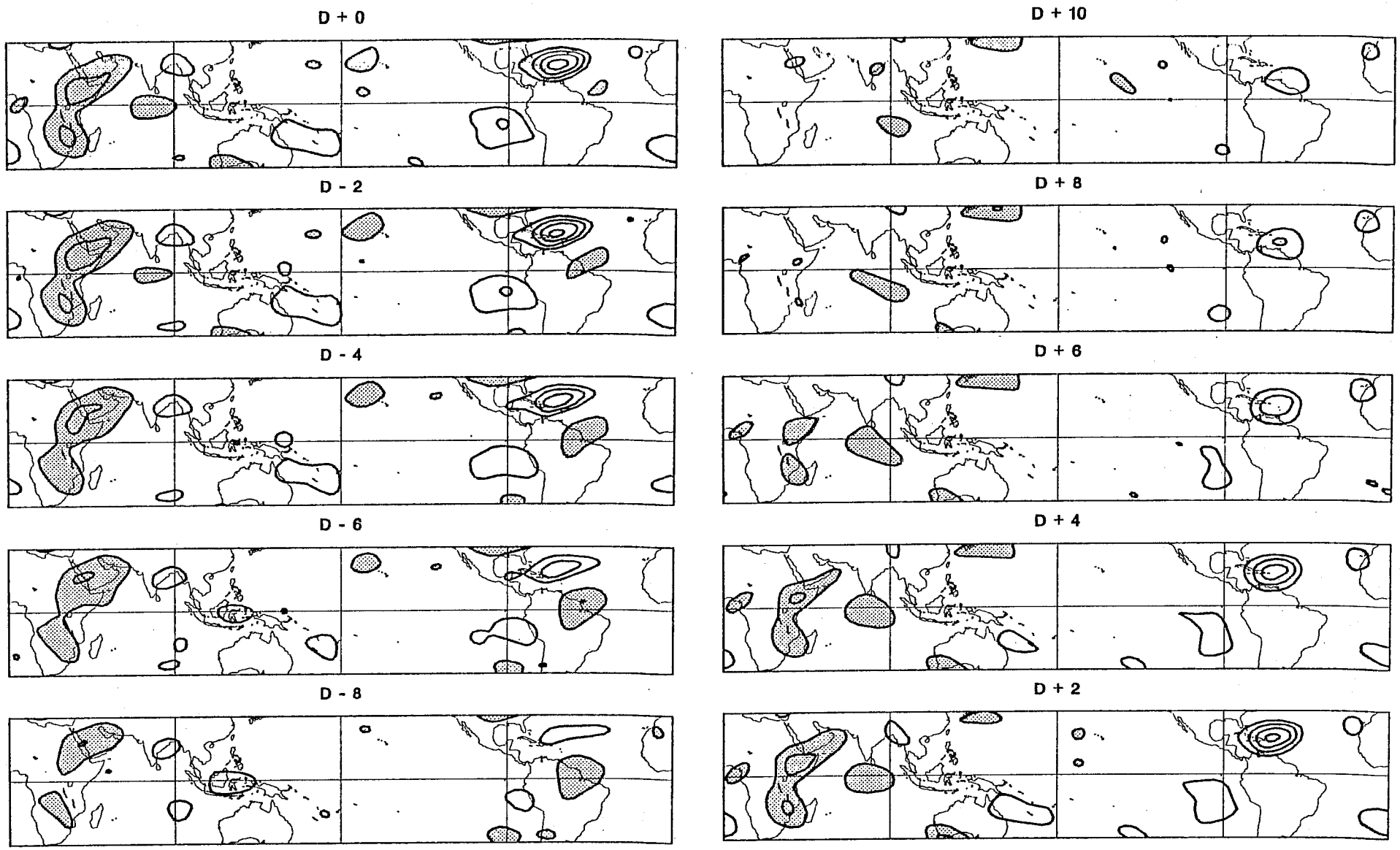

Fig. 8 Lead- and lag- correlations of the bandpass-filtered OLR time series at all the points in the tropics with that at the point 20N,65W, for the northern winter period only, based on data for the years 1981-87. The contours drawn are ±0.3, ±0.5, ±0.7... etc and values of less than -0.3 are shaded.

A well defined region of fairly large correlations over eastern Africa is seen both in Figs 7 and 8. The northern hemispheric portions of these structures appear to be associated with the continuation into the tropics of the wave-train depicted in Fig 6. There is the barest hint of this wave-train setting off a 40 to 50 day event in the Indian ocean.

In conclusion, although the synoptic time-scale transients of the Atlantic storm-track region were crucially important for the maintenance of the blocked regime over Europe in February 1986, there is evidence that reduced cloudiness and rainfall over the Caribbean area, and much more indirectly, unusual activity on the 40 to 50 day time scale in the western equatorial Pacific, may have contributed towards creating the conditions in the north Atlantic which made the blocking process more likely to occur.

Acknowledgements

The assistance of K. Arpe and L. Ferranti in processing the Outgoing Longwave Radiation data, kindly made available by Dr. P. Arkin of the Climate Analysis Center in Washington D.C., is gratefully acknowledged. The work described in Hoskins and Sardeshmukh (1987) was completed under the Joint Diagnostics Project of the University of Reading and the U.K. Meteorological Office that is concerned with studying the atmospheric general circulation using ECMWF data.

References

Blackmon, M.L., Lee, T.-H., Wallace, J.M., and H.-H. Hsu, 1984: Time variation of 500 mb height fluctuations with long, intermediate, and short time scales as deduced from lag-correlatio statistics. J. Atmos. Sci., 41, 981-991.

Duchon, C.E., 1979: Lanczos filtering in one and two dimensions. J. Appl. Meterorol., 18, 1016-1022.

Climate Analysis Center, 1985: Climate Diagnostics Bulletin, December 1985. National Meteorological Center, Washington.

Climate Analysis Center, 1986a: Climate Diagnostics Bulletin, January 1986. National Meteorological Center, Washington.

Climate Analysis Center, 1986b: Climate Diagnostics Bulletin, February 1986. National Meteorological Center, Washington.

Hoskins, B.J., and D.J. Karoly, 1981: The steady linear response of a spherical atmosphere to thermal and orographic forcing. J. Atmos. Sci., 38, 1179-1196.

Hoskins, B.J., James, I.N., and G.H. White, 1983: The shape, propagation, and mean-flow interaction of large-scale weather systems. J. Atmos. Sci., 40, 1595-1612.

Hoskins, B.J., McIntyre, M.E., and A.W. Robertson, 1985: On the use and significance of isentropic potential vorticity maps. Q.J.R. Meteorol. Soc., 111, 877-946.

Hoskins, B.J., and P.D. Sardeshmukh, 1987: A diagnostic study of the dynamics of the northern hemisphere winter of 1985-86. Q.J.R. Meteorol. Soc., 113, 759-778.

Sardeshmukh, P.D., and B.J. Hoskins, 1984: Spatial smoothing on the sphere. Mon. Weather Rev., 112, 2524-2529.

Shutts, G.J., 1986: A case study of eddy forcing during an Atlantic blocking episode. Advances in Geophysics, vol.29, pp 135-162.

Simmons, A.J., Wallace, J.M., and G.W. Branstator, 1983: Barotropic wave propagation and instability, and atmospheric teleconnection patterns. J. Atmos. Sci., 40, 1363-1392.

Wallace, J.M., and D.S. Gutzler, 1981: Teleconnections in the geopotential height field during the northern hemisphere winter. Mon. Weather Rev., 109, 785-812.

Weickmann, K.M., Lussky, G.R., and J.E. Kutzbach, 1985: A global-scale analysis of intraseasonal fluctuations of outgoing longwave radiation and 250 mb streamfunction during northern winter. Mon. Weather Rev., 113, 941-961.